JOURNAL OF GUIDANCE, CONTROL, AND DYNAMICS
Vol. 28, No. 5, September–October 2005

Boundary Feedback Control Using Proper Orthogonal Decomposition Models

R. Chris Camphouse*
Air Vehicles Directorate, Wright–Patterson Air Force Base, Ohio 45433

Reduced-order boundary feedback controls are obtained through weak formulations of proper orthogonal decomposition system models. Control gain information is used to determine model fidelity. A fixed-point iteration scheme is used to incorporate the reduced-order control in the full-order simulation for validation. The effectiveness of the reduced-order control on the reduced and full-order models is demonstrated.

Nomenclature

A, B	=	state and control matrices, respectively
K	=	feedback gain matrix
L	=	correlation matrix
Q, R	=	state and control weight matrices, respectively
S	=	solution snapshot
t	=	time
$\boldsymbol{x}$	=	spatial coordinate vector
α	=	reduced model temporal coefficient
$\dot{\alpha}$	=	$(\partial/\partial t)\alpha$
ϵ	=	conductivity constant
λ, v	=	eigenvalue and eigenvector, respectively
ϕ	=	reduced model basis mode

Subscript

0	=	initial value

Superscripts

n	=	index of current iterate
$'$,$''$	=	first- and second-order derivatives with respect to x

Introduction

At present, considerable research effort is concerned with feedback control law design for applications described by partial differential equations requiring very large systems for simulation. A particular example is feedback flow control. Fluid flows are described by the system of Navier–Stokes equations[1] with turbulence modeling required for high-Reynolds-number calculations.[2] Highly resolved flow solutions require systems describing thousands of states, possibly millions in the case of turbulent flow. Systematic development of feedback controls from systems such as these is a computationally intractable problem. The order of the system must be reduced before control law design is done.

Proper orthogonal decomposition (POD) is a popular order-reduction technique used to alleviate the computational expense required for simulation of very high-dimensional systems.[3–7] The snapshot method[8] is used to create an ensemble of solutions with open-loop control input data. The ensemble is used to construct a set of POD basis modes. Each mode is a linear combination of the snapshots. The modes maximize energy in the mean square sense.[9] Because of this, an energy argument is often used to determine model fidelity. From a given POD basis set, only the number of modes needed to contain a specified percentage of the total set energy are kept. This argument is problematic in the feedback control setting. Energy of POD modes generated from snapshots incorporating open-loop actuation might not correlate to the energy of the system under feedback control.

In many practical applications, boundary actuation is a requirement. The possibility of unmodeled dynamics in the system, or dynamics lost in the order reduction process, makes feedback control a requirement. Currently, systematic development of boundary feedback control laws from POD models is an open problem. Controls are often specified in an ad hoc way, developed for the case of interior distributed control, or simply specified through open-loop forcing. We aim to systematically develop boundary feedback controls from POD system models with verification done in the full-order simulation to ensure control effectiveness.

In the infinite-dimensional setting of feedback control of partial differential equations, feedback gain operators resulting from a linear-quadratic-regulator (LQR) control formulation can often be expressed in terms of an integral kernel called the functional gain.[10,11] Functional gains indicate states most significant to the control and provide information that can be used to guide sensor and control placement practices.[12,13] In this paper, we present an analogous idea to determine modes in a POD model that are most relevant to the control. Rather than relying on an energy argument to determine a POD basis set, we use the feedback gains of an LQR control formulation to determine the necessary modes in the reduced-order model. Only modes significant to the control law are kept, and they are used in the construction of the reduced-order control.

With a reduced-order POD model in hand, one can investigate the effectiveness of a control strategy by incorporating the control in the reduced-order model. However, control of the reduced-order model is not the "real" objective. Control of the physical system, or full-order simulation, with a control developed via a reduced-order model is really the desired outcome. In the case of boundary control, the control enters the system model through a boundary condition. For the specific case of an LQR Dirichlet boundary control formulation, system behavior on the interior of the domain determines the control at the boundary. To incorporate a reduced-order control in the full-order model, one has to project the full-order solution onto the POD basis,[14] which is defined on the entire domain. Specifying the boundary control beforehand in the full-order solution to obtain the correct projection onto the POD basis is difficult. We present an iterative scheme to do this projection.

To motivate the methods of this paper, consider the simple problem of controlled heat conduction on the unit interval. The dynamics of the system are described by the one-dimensional heat equation

$$\dot{w}(t,x) = \epsilon w''(t,x), \qquad t > 0, \quad x \in (0,1) \tag{1}$$

Received 3 May 2004; revision received 13 September 2004; accepted for publication 14 September 2004.

*Mathematician, 2210 Eighth Street, Building 146, Room 305, Control Design and Analysis Branch. Member AIAA.

with initial condition

$$w(0, x) = w_0(x) \tag{2}$$

By requiring Dirichlet boundary control, the boundary conditions for the system are specified as

$$w(t, 0) = u_0(t) \tag{3}$$

$$w(t, 1) = u_1(t) \tag{4}$$

where $u_0(t)$ is the control at $x = 0$ and $u_1(t)$ is the control at $x = 1$.

For this problem, boundary feedback control methods for distributed parameter systems are readily available to determine u_0 and u_1 (Ref. 15). However, in the context of boundary feedback control of reduced-order POD models, significant issues are unresolved even for this seemingly trivial problem. Questions to be resolved include the following:

1) How can a reduced-order POD model with explicit Dirichlet boundary control inputs be constructed in a form amenable to control law design?

2) What is the control objective for the system, and how is that formulated in terms of the reduced-order model?

3) What fidelity of the reduced-order model is needed to satisfy the control objective?

4) Is the feedback control obtained through order reduction effective in the reduced-order model?

5) How can the reduced-order control be implemented in the full-order system or simulation?

6) Is the reduced-order control effective in the full-order model?

This work attempts to answer these questions. We utilize system (1–4) as a specific example to enhance discussions of the methods of this paper. After the method has been fully described, we implement it for two-dimensional heat flow on a cavity geometry.

Model Development

An ensemble of solution snapshots $\{S_i(\boldsymbol{x})\}_{i=1}^N$ with nontrivial input data is generated. The $N \times N$ correlation matrix L defined by

$$L_{i,j} = \langle S_i, S_j \rangle \tag{5}$$

is constructed. In this work, we use the standard $L^2(\Omega)$ inner product

$$\langle S_i, S_j \rangle = \int_\Omega S_i S_j^* \, \mathrm{d}\boldsymbol{x} \tag{6}$$

where S_j^* denotes the complex conjugate of S_j, in the construction of L.

The eigenvalues of L are found. They are sorted in descending order, and their corresponding eigenvectors are calculated. Each eigenvector is normalized so that

$$\|v_i\|^2 = 1/\lambda_i \tag{7}$$

The orthonormal POD basis set is constructed according to

$$\phi_i(\boldsymbol{x}) = \sum_{j=1}^N v_{i,j} S_j(\boldsymbol{x}) \tag{8}$$

where $v_{i,j}$ is the jth component of v_i.

As the POD modes form an optimal basis for the snapshot ensemble in an energy sense, the true solution $w(t, \boldsymbol{x})$ of the distributed parameter system is approximated by a linear combination of the POD basis functions as

$$w(t, \boldsymbol{x}) \approx \sum_{i=1}^M \alpha_i(t) \phi_i(\boldsymbol{x}) \tag{9}$$

The sum in Eq. (9) is substituted into the governing partial differential equation model. Galerkin projection is done, and a system of ordinary differential equations for the temporal coefficients $\{\alpha_i(t)\}_{i=1}^M$ is developed. The initial condition specified for the temporal coefficients of the POD model is obtained by projecting the initial condition of the system onto the POD basis.

The order reduction method just described results in a model that can be simulated much more efficiently than the original full-order system. However, boundary conditions are not explicit. Boundary control inputs are made explicit by constructing the weak form of the POD model. To make this idea concise, we illustrate the technique for the simple system described by Eqs. (1–4).

Taking an inner product of both sides of Eq. (1) with $\phi_j(x)$ yields

$$\int_0^1 \dot{w}(t, x) \phi_j(x) \, \mathrm{d}x = \epsilon \int_0^1 w''(t, x) \phi_j(x) \, \mathrm{d}x \tag{10}$$

Integrating by parts results in the weak formulation

$$\int_0^1 \dot{w}(t, x) \phi_j(x) \, \mathrm{d}x = \epsilon \Bigg[w'(t, 0) \phi_j(1) - w'(t, 0) \phi_j(0) - \int_0^1 w'(t, x) \phi_j'(x) \, \mathrm{d}x \Bigg] \tag{11}$$

Control inputs are made explicit by approximating the boundary derivatives in Eq. (11). For $h > 0$, we see that

$$w'(t, 0) \approx [w(t, h) - w(t, 0)]/h = [w(t, h) - u_0(t)]/h \tag{12}$$

$$w'(t, 1) \approx [w(t, 1) - w(t, 1 - h)]/h = [u_1(t) - w(t, 1 - h)]/h \tag{13}$$

Substituting these approximations into Eq. (11) and writing $w(t, x)$ as a linear combination of POD modes results in

$$\dot{\alpha}_j = -\epsilon \sum_{i=1}^M \Bigg[\frac{\phi_j(1)}{h} \phi_i(1 - h) + \frac{\phi_j(0)}{h} \phi_i(h) + \int_0^1 \phi_i'(x) \phi_j'(x) \, \mathrm{d}x \Bigg] \alpha_i + \frac{\epsilon}{h} [\phi_j(0) u_0(t) + \phi_j(1) u_1(t)] \tag{14}$$

The system of ordinary differential equations given by Eq. (14) is written in the convenient state-space form $\dot{\alpha} = A\alpha + Bu$, where

$$A_{j,i} = -\epsilon \Bigg[\frac{\phi_j(1)}{h} \phi_i(1 - h) + \frac{\phi_j(0)}{h} \phi_i(h) + \int_0^1 \phi_i'(x) \phi_j'(x) \, \mathrm{d}x \Bigg] \tag{15}$$

$$B = \frac{\epsilon}{h} \begin{bmatrix} \phi_1(0) & \phi_1(1) \\ \cdot & \cdot \\ \cdot & \cdot \\ \cdot & \cdot \\ \phi_M(0) & \phi_M(1) \end{bmatrix}_{M \times 2} \tag{16}$$

Projecting the initial condition $w_0(x)$ onto the POD basis results in an initial condition for the reduced-order model of the form

$$\alpha(0) = \alpha_0 \tag{17}$$

Control Law Design

In this work, we are concerned with constructing boundary feedback control laws for finite-dimensional system models with state-space equations of the form

$$\dot{w} = Aw + Bu, \qquad t > 0 \tag{18}$$

$$w(0) = w_0(\boldsymbol{x}) \tag{19}$$

Equations (18) and (19) correspond to a linear system. However, when developing feedback controls for a nonlinear system model, a

linearization is often done, resulting in a system of the form given by Eqs. (18) and (19). The resulting linear state-space equation is then used to design control laws for the nonlinear system.[16–18]

We consider the tracking control problem for Eqs. (18) and (19). A fixed reference signal $z(\boldsymbol{x})$ is specified, and we desire that solutions of Eqs. (18) and (19) follow $z(\boldsymbol{x})$. Because the tracking signal is time invariant, the dynamics of the system under tracking control are given by

$$\begin{bmatrix} \dot{w} \\ \dot{z} \end{bmatrix} = \begin{bmatrix} A & 0 \\ 0 & 0 \end{bmatrix} \begin{bmatrix} w \\ z \end{bmatrix} + \begin{bmatrix} B \\ 0 \end{bmatrix} u \tag{20}$$

$$= \bar{A}X + \bar{B}u \tag{21}$$

where we have defined the augmented state X as

$$X(t, \boldsymbol{x}) = \begin{bmatrix} w(t, \boldsymbol{x}) \\ z(t, \boldsymbol{x}) \end{bmatrix} \qquad \text{with} \qquad X_0(\boldsymbol{x}) = \begin{bmatrix} w_0(\boldsymbol{x}) \\ z(\boldsymbol{x}) \end{bmatrix} \tag{22}$$

To formulate the control problem, we consider the tracking linear-quadratic-regulator cost function

$$J(w_0, u) = \int_0^\infty [(w - z)^T Q(w - z) + u^T Ru]\, \mathrm{d}t \tag{23}$$

In Eq. (23), Q is a diagonal, symmetric, positive semidefinite matrix of state weights. R is a diagonal, symmetric, positive-definite matrix of control weights. The optimal control problem we consider is to minimize Eq. (23) over all controls $u \in L^2(0, \infty)$ subject to the constraints (20–22).

For a controllable system, the tracking LQR problem has a unique solution of the form

$$u_{\text{opt}} = -KX \tag{24}$$

$$= -[K_1 \quad K_2]X \tag{25}$$

$$= -\left[R^{-1}B^T\Pi_{11} \quad R^{-1}B^T\Pi_{12}\right]X \tag{26}$$

where Π_{11} is the unique symmetric, nonnegative solution of the algebraic Riccati equation

$$A^T\Pi_{11} + \Pi_{11}A - \Pi_{11}BR^{-1}B^T\Pi_{11} + Q = 0 \tag{27}$$

The matrix Π_{12} in Eq. (26) satisfies the equation

$$\left[A^T - \Pi_{11}BR^{-1}B^T\right]\Pi_{12} = Q \tag{28}$$

The optimal feedback control law is placed into the augmented state-space equation. The resulting closed-loop system is of the form

$$\dot{X} = (\bar{A} - \bar{B}K)X \tag{29}$$

$$X(0) = X_0 \tag{30}$$

The tracking LQR formulation just discussed can be used to control the full-order model of the system as well as the reduced-order POD model with explicit control input. In the reduced-order case, the reference signal $z(\boldsymbol{x})$ is projected onto the POD modes to obtain reference coefficients $\{\bar{\alpha}_j\}_{j=1}^M$.

Validation

To validate the utility of the reduced-order control, it must be incorporated and tested in the full-order system. This requires that the reduced-order feedback gain matrix $\tilde{K}$ be placed in the closed-loop full-order system in an analogous way to Eq. (29). One cannot directly incorporate the reduced-order gain in the full-order system model, however. The gain obtained via the reduced-order model acts on the POD coefficients. As a result, one must project the full-order solution at each time step onto the POD modes. A technicality must be resolved when Dirichlet boundary controls resulting from a reduced-order POD model are to be used in the full-order system. The POD basis functions used to construct the reduced order model cover the entire domain, including the boundary. To project the full-order solution onto the POD basis set, boundary conditions must be specified for the full solution before the projection. As a result, to project the full-order solution with boundary data onto the POD modes the boundary control in the full-order solution must be specified beforehand, a seeming impossibility. We overcome this difficulty by using a fixed-point subiteration to project the full-order solution onto the POD basis at each time step. At $t = 0$, the full-order initial condition with boundary data is projected onto the POD basis to obtain projected initial temporal coefficients. For $t > 0$, two steps compose the fixed-point iteration.

Step 1

The coefficients from the preceding time step are used as an initial estimate of the coefficients at the current time step.

Step 2

Denote the current estimate of the projected coefficients by α^n. The boundary feedback control $u = -\tilde{K}[\alpha^n \quad \bar{\alpha}]^T$ is incorporated into the full-order solution. The full-order solution with control values at the boundary is projected onto the POD modes to obtain a new estimate for the temporal coefficients. Denote the new estimate by α^{n+1}. The quantity $\|\alpha^{n+1} - \alpha^n\|_\infty$ is calculated.

Step 2 is iterated until $\|\alpha^{n+1} - \alpha^n\|_\infty <$ tolerance, that is, the sequence of estimates of the projected POD coefficients for the current time step has converged. Denote the limit as α_L. Then, the closed-loop full-order system with the reduced-order feedback control is of the form

$$\dot{X} = \bar{A}X - \bar{B}\tilde{K}[\alpha_L \quad \bar{\alpha}]^T \tag{31}$$

$$X(0) = X_0 \tag{32}$$

where X is comprised of the state variables in the high-order tracking system.

Implementation

We are now in a position to solidify the techniques discussed to this point by implementing them for the system described by Eqs. (1–4). In the results that follow, the initial condition specified is $w_0(x) = \sin(\pi x)$. The value specified for the conductivity constant is $\epsilon = 0.1$.

POD Model

We numerically simulate system (1–4) to obtain an ensemble of solution snapshots. Second-order accurate finite difference approximations are used to discretize spatial derivatives in the full-order simulation. Time integration is done with a fourth-order Runge–Kutta method. As the resulting POD basis modes are to be used for feedback boundary control, nontrivial boundary inputs are specified during the snapshot generation process. The boundary inputs we specify are of the form

$$u_0(t) = 0, \qquad u_1(t) = 0 \tag{33}$$

$$u_0(t) = 0.25\sin(n\pi t), \qquad u_1(t) = 0 \tag{34}$$

$$u_0(t) = 0, \qquad u_1(t) = 0.25\sin(n\pi t) \tag{35}$$

The values specified for n in Eqs. (34) and (35) are 0.25, 0.5, 0.75, and 1. In the snapshots resulting from Eq. (33), the initial condition is evolved to a steady state. The snapshots generated by Eq. (34) capture dynamics resulting from the left control under various inputs. Similarly, the snapshots generated by Eq. (35) capture dynamics resulting from the right control. The solution snapshots generated with the boundary inputs given by Eqs. (33–35) are used to generate a set of POD modes. The first eight POD modes obtained are shown in Fig. 1.

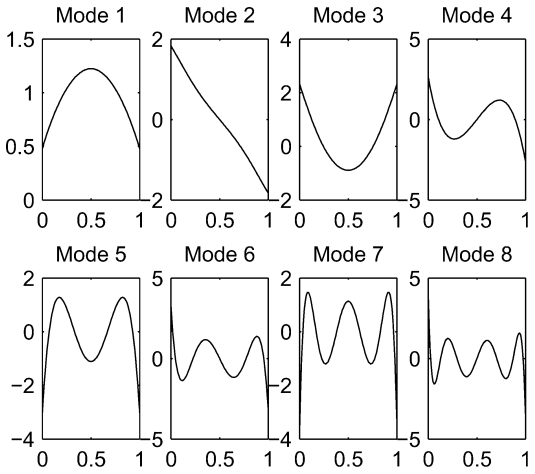

Fig. 1 POD modes for the one-dimensional problem.

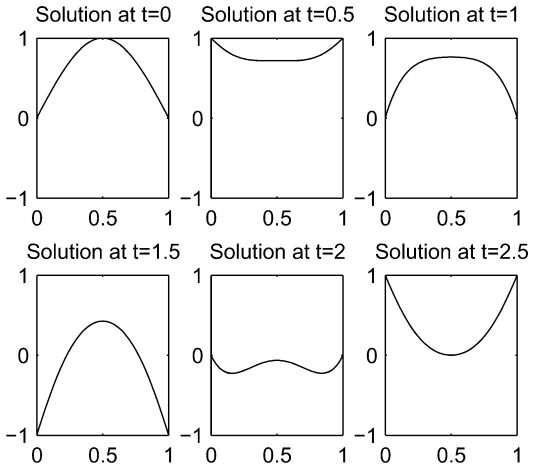

Fig. 2 Model comparison, $u_0(t) = u_1(t) = \sin(\pi t)$.

As shown earlier, the reduced-order model of this system is of the form

$$\dot{\alpha} = A\alpha + Bu, \qquad t > 0 \tag{36}$$

$$\alpha(0) = \alpha_0 \tag{37}$$

where A is defined by Eq. (15), B is defined by Eq. (16), and α_0 is obtained by projecting the initial condition $w_0(x)$ onto the POD basis.

Before using the reduced-order model to develop feedback controls for the system, we verify that results obtained from the reduced-order model and the full-order simulation are in good agreement. To do this, we specify $u_0(t)$ and $u_1(t)$ as open-loop, time-varying boundary conditions and compare solutions obtained from the POD model with those obtained from the full-order simulation. We specify that both control inputs are nonzero. Specifying the inputs in this way demonstrates the robustness of the reduced-order model because it is a case not considered in the construction of the snapshot ensemble. The values we specify for the control inputs are $u_0(t) = \sin(\pi t)$ and $u_1(t) = \sin(\pi t)$. The results from this case are shown in Fig. 2. In Fig. 2, solid curves denote the solution of the full-order simulation. Dashed curves represent solutions of the reduced-order model. The curves are coincident. Very good agreement is achieved for this case, even though it is not included in the conditions specified during snapshot generation. Now that we are confident in the POD model, we are ready to use it for control law design.

Feedback Control

We construct a tracking LQR boundary feedback control from the reduced-order POD model. We specify the reference function

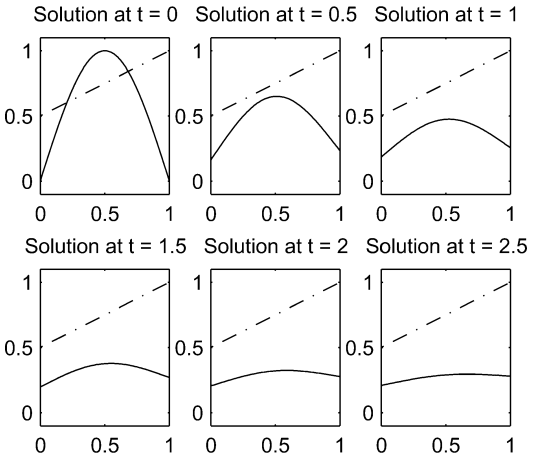

Fig. 3 Controlled reduced-order model, $Q = I^{8\times 8}$.

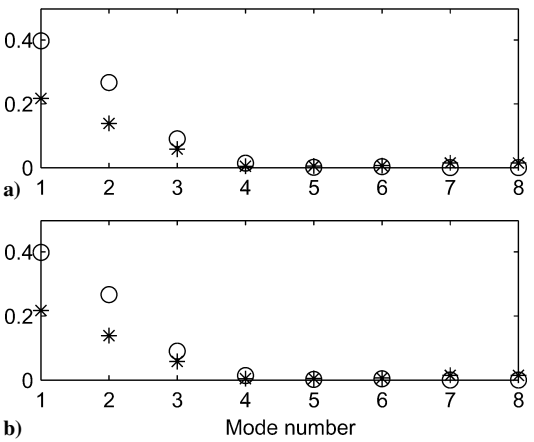

Fig. 4 Gain magnitudes for a) $u_0(t)$ and b) $u_1(t)$.

$z(x)$ as

$$z(x) = 0.5x + 0.5 \tag{38}$$

The reference function is projected onto the POD basis modes of Fig. 1. A trapezoid integration rule is used for the numerical spatial integrations needed in the projection. The coefficients resulting from the projection are used as tracking coefficients in the reduced-order model. For the reduced-order control problem, we specify the control weight matrix R as the 2×2 identity matrix. We initially specify the state weight matrix Q to be the 8×8 identity matrix. The resulting tracking LQR problem is solved. The behavior of the closed-loop reduced-order model is shown in Fig. 3.

From Fig. 3, it is apparent that the control obtained by specifying Q as the 8×8 identity matrix is not effective. The solution obtained for the reduced-order model does not track the reference function, indicated by the dashed line. However, the gains obtained by solving the control problem indicate which states in the reduced-order model are most significant to the control. The magnitudes of the gains K_1 and K_2, defined by Eqs. (25) and (26), are depicted in Fig. 4 by asterisks and circles, respectively.

As seen in Fig. 4, the first three POD coefficients are most significant to the control problem. The magnitudes of the gains are greatest for the first three modes for both controls. With this information in hand, we discard all modes except the first three. Their temporal coefficients are each given a state weight of 1000. The behavior of the resulting closed-loop reduced-order model is illustrated in Fig. 5. As seen in that figure, the reduced-order model consisting of only the first three modes satisfies the control objective quite well.

Validation

Now that the control objective has been sufficiently demonstrated for the reduced-order POD model, we incorporate the reduced-order

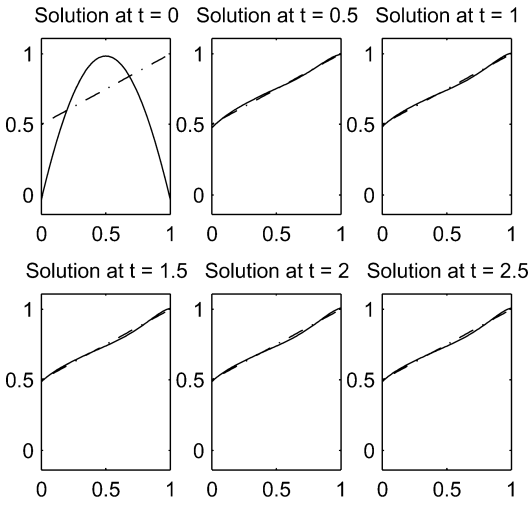

Fig. 5 Controlled three-mode POD model.

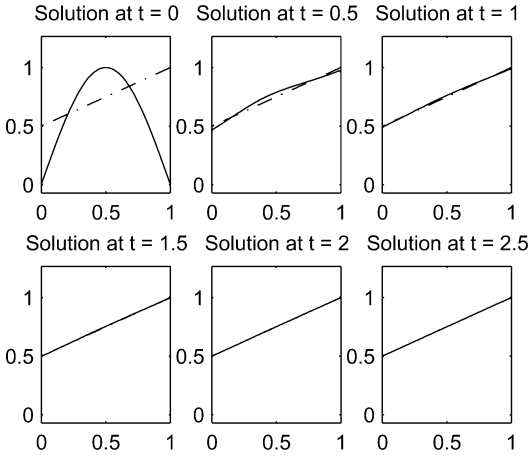

Fig. 6 Controlled full-order simulation with the reduced-order gain.

control in the full-order simulation to validate its effectiveness in the real problem. The fixed-point iteration scheme discussed earlier is used to project the full-order solution onto the set of POD modes at each time step. The closed-loop full-order simulation is shown in Fig. 6. From Fig. 6, it is clear that tracking is achieved when the reduced-order gain resulting from the three-mode POD model is incorporated into the full-order simulation.

As the full-order system is not exceedingly large, we apply the LQR techniques utilized thus far to it. Each state is given a state weight of 1000. The resulting control problem is solved, and a full-order gain is obtained. The closed-loop behavior of the full-order system with a full-order control is shown in Fig. 7. The results of Figs. 6 and 7 are indistinguishable. The reduced-order control provided by the three-mode POD model is able to track the reference signal as well as a full-order control obtained via full state feedback, the best possible case.

Model Problem: Two-Dimensional Cavity

We now extend the techniques of this paper to a system described on a two-dimensional geometry of the kind seen in cavity noise reduction applications. To develop the partial differential equation model of the system, define the real-valued constants a_1, a_2, a_3, and a_4 according to $a_1 < a_2 < a_3 < a_4$. Similarly, define the constants b_1, b_2, and b_3 according to $b_1 < b_2 < b_3$. Define the regions Ω_1 and Ω_2 according to

$$\Omega_1 = (a_1, a_4) \times (b_2, b_3), \qquad \Omega_2 = (a_2, a_3) \times (b_1, b_2] \tag{39}$$

The problem domain Ω is given by

$$\Omega = \Omega_1 \cup \Omega_2 \tag{40}$$

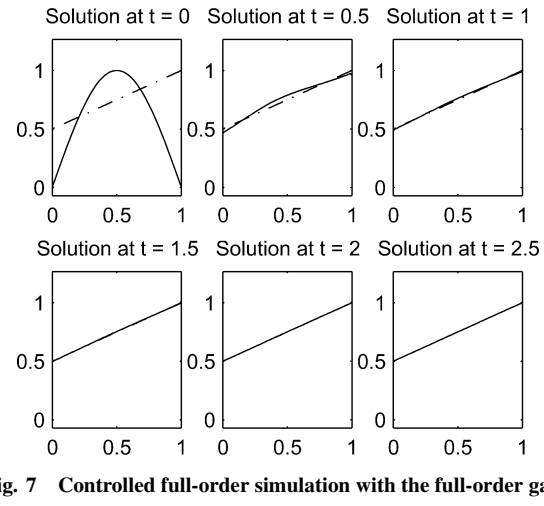

Fig. 7 Controlled full-order simulation with the full-order gain.

In this configuration, Ω_2 is the cavity on which we incorporate Dirichlet boundary control. In particular, controls are located on the forward and rear cavity walls, which are denoted by Γ_F and Γ_R, respectively.

The dynamics of the system are given by the two-dimensional heat equation

$$\frac{\partial}{\partial t} w(t, x, y) = \epsilon \left[\frac{\partial^2}{\partial x^2} w(t, x, y) + \frac{\partial^2}{\partial y^2} w(t, x, y) \right] \tag{41}$$

for $t > 0$ and $(x, y) \in \Omega$.

For simplicity, we specify that the controls on Γ_F and Γ_R are separable, that is, they are a product of a function of time and a function of the spatial variables. The resulting boundary conditions on the forward and rear cavity walls are of the form

$$w(t, \Gamma_F) = u_F(t) \Psi_F(y) \tag{42}$$

$$w(t, \Gamma_R) = u_R(t) \Psi_R(y) \tag{43}$$

In Eqs. (42) and (43), u_F and u_R are the controls on the forward and rear cavity walls, respectively. The profile functions Ψ_F and Ψ_R describe the influence of the controls on the boundary.

For notational convenience denote the remaining domain boundary by Γ_U. We specify that values on Γ_U be held at zero as time evolves. The resulting boundary condition is of the form

$$w(t, \Gamma_U) = 0 \tag{44}$$

To complete the model, we specify an initial condition of the form

$$w(0, x, y) = w_0(x, y) \in L^2(\Omega) \tag{45}$$

POD Model

As in the one-dimensional example, we numerically simulate system (41), (42–45) in order to obtain an ensemble of solution snapshots. Second-order-accurate finite difference approximations are used to discretize spatial derivatives in the full-order simulation. Time integration is done with a fourth-order Runge–Kutta method. The values we specify for a_1, a_2, a_3, and a_4 are 0, 0.2, 0.4, and 0.6, respectively. Similarly, the quantities b_1, b_2, and b_3 are specified as 0, 0.1, and 0.35. The conductivity constant ϵ is set to $\epsilon = 0.01$. The control profile functions Ψ_F and Ψ_R are defined according to

$$\Psi_{F,R}(y) = \begin{cases} 1, & y \in [0.05, 0.1] \\ 0, & \text{otherwise} \end{cases} \tag{46}$$

As the snapshots are to be used to construct a POD model amenable to boundary control law design, nontrivial control inputs

are specified during the snapshot generation process. The boundary inputs we specify are of the form

$$u_F(t) = 0, \qquad u_R(t) = 0, \tag{47}$$

$$u_F(t) = 0.5\sin(n\pi t), \qquad u_R(t) = 0 \tag{48}$$

$$u_F(t) = 0, \qquad u_R(t) = 0.5\sin(n\pi t) \tag{49}$$

$$u_F(t) = 0.5\sin(n\pi t), \qquad u_R(t) = 0.5\sin(n\pi t) \tag{50}$$

The values specified for n in Eqs. (47–50) are $n = 0.2, 0.4, 0.6, 0.8$, and 1. In the snapshots generated from Eq. (47), the initial condition is evolved to a steady state. The first six POD modes obtained are shown in Fig. 8.

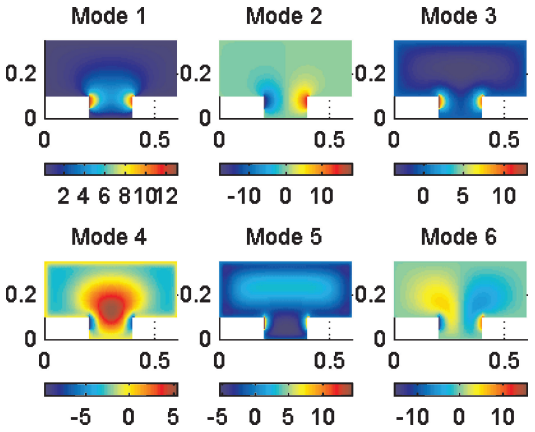

Fig. 8 POD modes for the cavity problem.

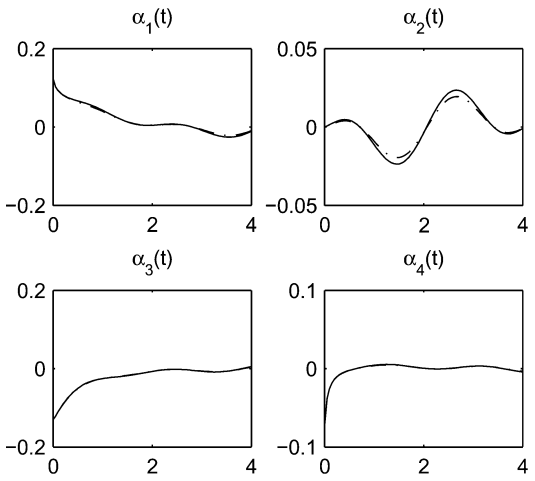

Fig. 9 Projected and POD model coefficients.

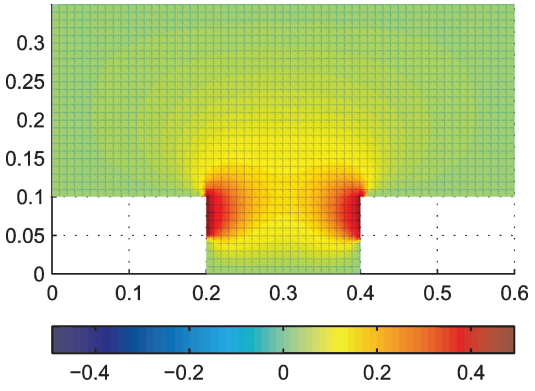

Fig. 10 Reference function from a two-mode projection.

We now construct a reduced-order model of the system with explicit control input. Taking the inner product of both sides of governing equation (41) with $\phi_j(x, y)$ yields

$$\int_\Omega \frac{\partial}{\partial t} w(t, x, y)\phi_j(x, y)\,\mathrm{d}\boldsymbol{x} = \epsilon \int_\Omega \left[\frac{\partial^2}{\partial x^2} w(t, x, y) + \frac{\partial^2}{\partial y^2} w(t, x, y)\right]\phi_j(x, y)\,\mathrm{d}\boldsymbol{x} \tag{51}$$

Utilizing Green's identity, Eq. (51) is written weakly as

$$\int_\Omega \frac{\partial}{\partial t} w(t, x, y)\phi_j(x, y)\,\mathrm{d}\boldsymbol{x} = \epsilon\left\{\int_{\partial\Omega} \phi_j(x, y)[\nabla w(t, x, y)\cdot \boldsymbol{n}] \times \mathrm{d}A(\boldsymbol{x}) - \int_\Omega \nabla w(t, x, y)\cdot\nabla\phi_j(x, y)\,\mathrm{d}\boldsymbol{x}\right\} \tag{52}$$

where $\boldsymbol{n}$ is the unit outward normal.

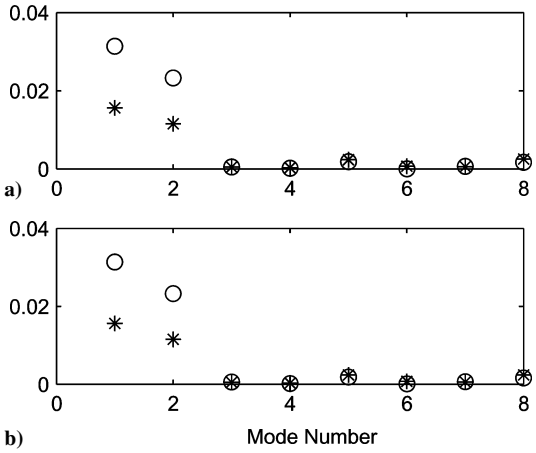

Fig. 11 Gain magnitudes for a) $u_F(t)$ and b) $u_R(t)$.

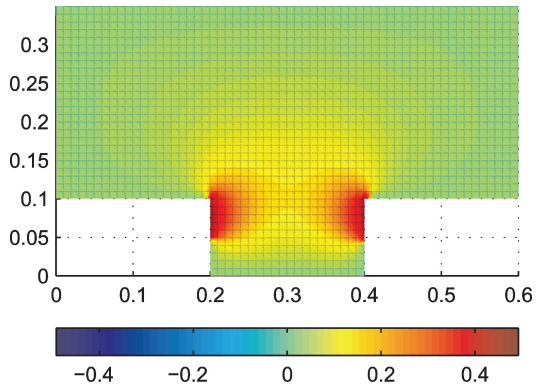

Fig. 12 Steady-state controlled two-mode POD model.

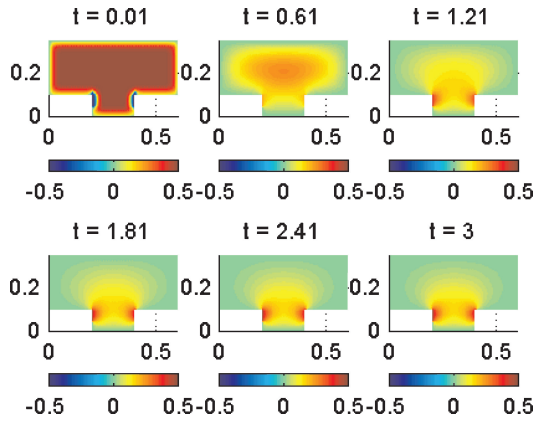

Fig. 13 Controlled full-order simulation with reduced-order gain.

As the boundary domain is specified to be zero everywhere except for the forward and rear cavity walls,

$$\int_{\partial\Omega} \phi_j(x, y)[\nabla w(t, x, y) \cdot \boldsymbol{n}]\, \mathrm{d}A(\boldsymbol{x})$$

$$= \int_{\Gamma_F} \phi_j(x, y)[\nabla w(t, x, y) \cdot \boldsymbol{n}]\, \mathrm{d}A(\boldsymbol{x})$$

$$+ \int_{\Gamma_R} \phi_j(x, y)[\nabla w(t, x, y) \cdot \boldsymbol{n}]\, \mathrm{d}A(\boldsymbol{x}) \tag{53}$$

$$= -\int_{b_1}^{b_2} \phi_j(a_2, y) \frac{\partial}{\partial x} w(t, a_2, y)\, \mathrm{d}y$$

$$+ \int_{b_1}^{b_2} \phi_j(a_3, y) \frac{\partial}{\partial x} w(t, a_3, y)\, \mathrm{d}y \tag{54}$$

As before, we obtain explicit control inputs by approximating partial derivatives of $w(t, x, y)$ at the forward and rear cavity walls. For $h > 0$, we have

$$\frac{\partial}{\partial x} w(t, a_2, y) \approx \frac{w(t, a_2 + h, y) - w(t, a_2, y)}{h}$$

$$= \frac{w(t, a_2 + h, y) - u_F(t)\Psi_F(y)}{h} \tag{55}$$

$$\frac{\partial}{\partial x} w(t, a_3, y) \approx \frac{w(t, a_3, y) - w(t, a_3 - h, y)}{h}$$

$$= \frac{u_R(t)\Psi_R(y) - w(t, a_3 - h, y)}{h} \tag{56}$$

Substituting these approximations into Eq. (54) and writing $w(t, x, y)$ as a linear combination of POD modes in Eq. (52) yields

$$\dot{\alpha_j}(t) = \frac{\epsilon}{h}\left[u_R(t) \int_{b_1}^{b_2} \phi_j(a_3, y)\Psi_R(y)\, \mathrm{d}y \right.$$

$$\left. + u_F(t) \int_{b_1}^{b_2} \phi_j(a_2, y)\Psi_F(y)\, \mathrm{d}y \right] - \frac{\epsilon}{h} \sum_{i=1}^{M} \left\{ \int_{b_1}^{b_2} [\phi_j(a_3, y) \right.$$

$$\times \phi_i(a_3 - h, y) + \phi_j(a_2, y)\phi_i(a_2 + h, y)]\, \mathrm{d}y$$

$$\left. + h \int_{\Omega} \nabla\phi_j(x, y) \cdot \nabla\phi_i(x, y)\, \mathrm{d}\boldsymbol{x} \right\} \alpha_i(t) \tag{57}$$

The system of ordinary differential equations given by Eq. (57) is written in the state-space form $\dot{\alpha} = A\alpha + Bu$, where

$$A_{j,i} = -\frac{\epsilon}{h}\left\{ \int_{b_1}^{b_2} [\phi_j(a_3, y)\phi_i(a_3 - h, y) + \phi_j(a_2, y) \right.$$

$$\left. \times \phi_i(a_2 + h, y)]\, \mathrm{d}y + h \int_{\Omega} \nabla\phi_j(x, y) \cdot \nabla\phi_i(x, y)\, \mathrm{d}\boldsymbol{x} \right\} \tag{58}$$

$$B = \frac{\epsilon}{h} \begin{bmatrix} \int_{b_1}^{b_2} \phi_1(a_2, y)\Psi_F(y)\, \mathrm{d}y & \int_{b_1}^{b_2} \phi_1(a_3, y)\Psi_R(y)\, \mathrm{d}y \\ \vdots & \vdots \\ \int_{b_1}^{b_2} \phi_M(a_2, y)\Psi_F(y)\, \mathrm{d}y & \int_{b_1}^{b_2} \phi_M(a_3, y)\Psi_R(y)\, \mathrm{d}y \end{bmatrix}_{M \times 2} \tag{59}$$

As before, the initial condition for the reduced-order model is obtained by projecting $w_0(x, y)$ onto the POD basis.

We now verify that results obtained from the reduced- and full-order models are in good agreement. The full-order solution at each time step is projected onto the POD basis. The resulting temporal coefficients are compared to those obtained from the reduced-order model. In both simulations, we specify open-loop control inputs of the form $u_F(t) = 0.5 \sin(0.5\pi t)$ and $u_R(t) = 0.5 \sin(\pi t)$. None of the snapshots created during the ensemble creation process include boundary inputs of this form. The temporal coefficients obtained for the first four modes are shown in Fig. 9. In Fig. 9, solid curves denote projected coefficients while dashed curves represent coefficients obtained from the reduced-order model. As is evident, very good agreement is seen between the reduced- and full-order simulations, even though the boundary inputs specified are different than those chosen during ensemble creation.

Feedback Control

Now that we are confident in the reduced-order model, we utilize it for tracking boundary feedback control. To construct a reference function in the results that follow, we specify a globally defined function $f(x, y)$ according to

$$f(x, y) = \begin{cases} 0.5, & (x, y) \in [0.2, 0.4] \times [.05, 0.1] \\ 0, & \text{otherwise} \end{cases} \tag{60}$$

We then project $f(x, y)$ onto the set of POD modes to obtain the reference function $z(x, y)$. The reference function obtained by projecting $f(x, y)$ onto the first two POD modes is shown in Fig. 10.

We follow the same procedure as before to determine which POD modes are most significant to the control problem. We initially construct the matrix of state weights as $Q = I^{8\times 8}$. We specify the matrix of control weights to be $R = I^{2\times 2}$. The resulting tracking LQR problem is solved, and a feedback gain matrix K is obtained.

As in the one-dimensional case, the control obtained by specifying Q as the 8×8 identity matrix is not effective. The solution obtained for the reduced-order model does not track the reference function. The magnitudes of the gains K_1 and K_2, defined by Eq. (25) and (26), are depicted in Fig. 11 by asterisks and circles, respectively. As evident in Fig. 11, the first two POD modes have the greatest contribution to the controls. With this information in hand, we discard all modes except the first two. The first two modes are given a state weight of 10,000. The resulting steady-state solution of the controlled reduced-order model is shown in Fig. 12.

By comparing the controlled solution of Fig. 12 with the reference signal shown in Fig. 10, it is clear that the control objective is achieved. The controlled reduced-order model and the reference function are virtually identical.

Validation

Now that the control objective has been attained for the reduced-order POD model, we implement the reduced-order control in the full-order simulation. The reduced-order gain obtained from the control problem for the POD model consisting of two modes with state weights of 10,000 is used to control the full-order simulation. The resulting closed-loop full-order simulation is shown in Fig. 13.

The reduced-order control is very effective when implemented in the full-order simulation. The full-order solution tracks the reference signal very well, as evident by comparing the steady-state solution of Fig. 13 with the two-mode reference function of Fig. 10.

Conclusions

The effectiveness of boundary feedback controllers developed from simulation-based proper orthogonal decomposition models has been demonstrated. Optimal feedback controllers were obtained for reduced-order models of the one-dimensional heat equation on an interval and the two-dimensional heat equation on a cavity geometry. Dirichlet boundary control was specified in both cases. The feedback controllers obtained were able to satisfy the tracking objectives very well. Effective tracking was seen in the controlled reduced-order models. When the reduced-order controls were incorporated into the full-order simulation, excellent tracking was seen there as well.

In both the one-dimensional and two-dimensional configurations, models consisting of three modes or less were sufficient in developing an effective control when gain information was used to determine model fidelity. These results provide a critical first step in the application of boundary feedback control to fluid flow applications where optimal feedback control design from the full-order system is a computationally intractable problem. Control design from reduced-order flow models has the potential of making systematic control design a feasible approach for practical flow control applications.

References

[1]Batchelor, G., *An Introduction to Fluid Dynamics*, Cambridge Univ. Press, New York, 1967, pp. 399–352.

[2]Fletcher, C., *Computational Techniques for Fluid Dynamics*, Vol. 2, Springer-Verlag, New York, 2003, pp. 399–352.

[3]Carabello, E., Samimy, M., and DeBonis, J., "Low Dimensional Modeling of Flow for Closed-Loop Flow Control," AIAA Paper 2003-0059, Jan. 2003.

[4]Carlson, H., Glauser, M., Higuchi, H., and Young, M., "POD Based Experimental Flow Control on a NACA-4412 Airfoil," AIAA Paper 2004-0575, Jan. 2004.

[5]Carlson, H., Glauser, M., and Roveda, R., "Models for Controlling Airfoil Lift and Drag," AIAA Paper 2004-0579, Jan. 2004.

[6]Cohen, K., Siegal, S., McLaughlin, T., and Myatt, J., "Proper Orthogonal Decomposition Modeling of a Controlled Ginzburg-Landau Cylinder Wake Model," AIAA Paper 2003-2405, Jan. 2003.

[7]Efe, M., and Ozbay, H., "Proper Orthogonal Decomposition for Reduced Order Modeling: 2D Heat Flow," *Proceedings of IEEE International Conference on Control Applications* (to be published).

[8]Sirovich, L., "Turbulence and the Dynamics of Coherent Structures, Parts I–III," *Quarterly of Applied Mathematics*, Vol. 45, No. 3, 1987, pp. 561–590.

[9]Holmes, P., Lumley, J., and Berkooz, G., *Turbulence, Coherent Structures, Dynamical Systems and Symmetry*, Cambridge Univ. Press, New York, 1996, pp. 86–127.

[10]Bensoussan, A., Prato, G., Delfour, M., and Miller, S., "Representation and Control of Infinite Dimensional Systems," *Systems & Control: Foundations & Applications*, Vol. 2, Birkhauser, Boston, 1992, pp. 259–317.

[11]Hulsing, K., "Numerical Methods for Approximating Functional Gains for LQR Control of Partial Differential Equations," Ph.D. Dissertation, Dept. of Mathematics, Virginia Polytechnic Inst. and State Univ., Blacksburg, VA, Dec. 1999, pp. 23–40.

[12]Borggaard, J., and Burns, J., "A Continuous Control Design Method," AIAA Paper 2002-2998, June 2002.

[13]Borggaard, J., Burns, J., and Zietsman, L., "Computational Challenges in Control of Partial Differential Equations," AIAA Paper 2004-2526, June 2004.

[14]Banks, H., del Rosario, R., and Smith, R., "Reduced Order Model Feedback Control Design: Numerical Implentation in a Thin Shell Model," Center for Research in Scientific Computation, North Carolina State Univ., Technical Rept. CRSC-TR98-27, Raleigh, June 1998.

[15]Lasiecka, I., and Triggiani, R., *Control Theory for Partial Differential Equations: Continuous and Approximation Theories*, Vol. 1, Cambridge Univ. Press, New York, 2000, pp. 178–194.

[16]Burns, J., and Kang, S., "A Control Problem for Burgers Equation with Bounded Input/Output," *Nonlinear Dynamics*, Vol. 2, Kluwer Academic, Norwell, MA, 1991, pp. 235–262.

[17]Burns, J., and Kang, S., "A Stabilization Problem for Burgers Equation with Unbounded Control and Observation," *Control and Estimation of Distributed Parameter Systems*, Vol. 100, Birkhauser Verlag, Basel, 1991, pp. 51–72.

[18]Camphouse, R., and Myatt, J., "Feedback Control for a Two-Dimensional Burgers Equation System Model," AIAA Paper 2004-2411, June 2004.